Investigating the stability of cyclopropylamine-based plasma polymers in water

Ke Vin Chan[1], Yuliia Onyshchenko[1], Mahtab Asadian[1], Anton Yu Nikiforov[1], Heidi Declercq[2,3], Rino Morent[1], Nathalie De Geyter[1]*

[1]Research Unit Plasma Technology (RUPT), Department of Applied Physics, Faculty of Engineering and Architecture, Ghent University, Sint-Pieternieuwstraat 41, B4, 9000 Ghent, Belgium

[2]Tissue Engineering Lab, Department of Development and Regeneration, Faculty of Medicine, KU Leuven Kulak, Herestraat 49, Box 805, 3000 Leuven, Belgium

[3]Tissue Engineering Group, Department of Human Structure and Repair, Faculty of Medicine and Health Sciences, Ghent University, De Pintelaan 185, B3, 9000 Ghent, Belgium

Abstract

Amino-rich thin coatings, known to show superior cell adhesion, proliferation and viability, are prepared in this study by means of plasma polymerization. The Yasuda parameter (W/FM) is used as a scaling factor for the deposition of cyclopropylamine based plasma polymer films (CPA-PPFs) using a dielectric barrier discharge (DBD) operated at sub-atmospheric pressure. This experimental research focusses on the stability of the CPA-PPFs in water. The polymerized samples are immersed in water for 24 h after which the coatings are chemically evaluated using Fourier transform infrared (FTIR) and X-ray photoelectron (XPS) spectroscopy. The results reveal that for all examined W/FM values water immersion results in a significant loss in C=N/C≡N groups and a shift of primary to secondary/tertiary amines

combined with the incorporation of oxygen as amides and alcohols/ethers. FTIR, XPS depth profiling and scanning electron microscopy (SEM) results reveal that at W/FM values ≤ 288 MJ/kg, the PPFs are gradually dissolving during water immersion, while at higher values, the PPFs are delaminating from the substrate due to their high crosslinking degree. Nevertheless, cell-coating interaction studies reveal no signs of cytotoxicity 1 day after cell seeding and show that remained thin coatings on the substrate strongly increase the adhesion of fibroblasts.

Keywords

Non-thermal plasma, plasma polymerisation, stability, cell study, XPS C_{60} depth profiling

1. Introduction

Plasma surface modification technologies have been extensively used to selectively incorporate desired functional groups onto polymeric surfaces to enhance cellular proliferation and adhesion [1–3]. For any given functional group to be incorporated, there is a multitude of plasma discharges which can be applied using many different combinations of discharge gases and/or monomer precursors. For example, the exposure of polymer surfaces to oxygen, ammonia or nitrogen plasma results in free radical substitution reactions also known as grafting leading to the incorporation of oxygen and nitrogen functionalities at the surface of polymer surfaces. Another applied strategy is plasma polymerisation which can be achieved by introducing a precursor containing the desired functional group into the plasma discharge to be plasma polymerised into a thin organic film on the surface of the polymeric substrate [4–8]. Moreover, depending on the type of plasma used, plasma exposure may have a surface smoothening effect which is known to further increase the biocompatibility of the polymeric substrate [9]. Indeed, many studies have shown that cells which were cultured on smoother surfaces demonstrated a significant increase in cell adhesion and proliferation, an increase in

organised actin filament formation and higher contact between the substrate surface and cell membranes when compared to rough surfaces [9–11].

Among various functional groups of interest for biomedical applications, amino ($–NH_2$) functionalised surfaces have shown very promising results as they elicit positive cell-surface interactions [12–14]. Under the appropriate conditions, it has already been shown that $–NH_2$ protonation is able to electrostatically immobilize DNA via its negatively charged phosphate backbone [4,15–19]. Additionally, amino functionalised surfaces can also be easily activated using inexpensive glutaraldehyde for protein immobilisation and this in a more efficient manner compared to carboxylic groups (-COOH), which are also often examined in the biomedical field [20]. Previous studies have already shown that amino functionalised polymer surfaces can be more efficiently obtained using plasma polymerisation of amino-containing precursors (allylamine, ethylenediamine, …) than by using plasma activation approaches [21–23]. Regardless of the plasma polymerisation route taken for the deposition of amino-rich coatings, it is important for biomedical applications to investigate the stability of the deposited films in an aqueous environment to avoid any potential toxic solvate that could negatively affect cellular activity during cell culturing. Unfortunately, the aqueous stability requirement of amino-rich plasma polymer films (PPFs) has been shown to be notoriously difficult to achieve without compromising on retaining a high concentration of amino functional groups. This is due to the fact that to deposit an adequately crosslinked, highly stable amino-rich PPF, a high discharge power is typically needed causing the precursor to be highly fragmented which inevitably destroys the desired amino functional groups. Numerous experiments using precursors such as ethylenediamine, allylamine or a mixture of ethylene and ammonia have demonstrated the problematic phenomenon of poor aqueous stability of amino-rich PPFs [4,14,24–26]. Experiments performed by Truica-Marasescu et al. [14] and Ruiz et al. [25] revealed that by using a high flow rate of ethylene compared to NH_3, the PPFs deposited at

atmospheric pressure showed a significantly lower nitrogen and amino content. Nevertheless, these PPFs did show a significantly lower loss in thickness when submerged in water compared to PPFs prepared at low ethylene flow rate or low discharge pressure. Literature also revealed that the stability of amino-rich PPFs is also greatly affected by the precursor type chosen for PPF deposition. Using the same plasma set-up and the same plasma operational parameters, amino-rich PPFs deposited using allylamine were comparatively more stable than PPFs prepared from ethylenediamine [27].

In our previous work, plasma polymerization experiments of cyclopropylamine (CPA) using a dielectric barrier discharge (DBD) sustained in argon at sub-atmospheric pressure have been conducted. Results showed that using CPA as precursor, amino-rich PPFs were successfully deposited on polyethylene (PE) substrates containing varying concentrations of –NH_2 groups when changing the Yasuda parameter (W/FM) which is the ratio between the applied discharge power (W) and the product of the monomer flow rate (F) and the molecular weight of the monomer (M) [28,29]. Within this previously published paper, experimental work was limited to the examination of the chemical and physical properties of the developed amino-rich PPFs immediately after conducting the plasma polymerization experiments. However, in this paper, this preliminary study will be further elaborated by profoundly investigating the film chemistry and the physical stability of the fabricated CPA-based PPFs after submerging the plasma deposits in an aqueous environment for 24 h. To investigate the film chemistry, this study will include the use of Fourier transform infrared spectroscopy (FTIR) and X-ray photoelectron spectroscopy (XPS) as such and in combination with 4-trifluoromethyl benzaldehyde (TFBA) derivatization, the latter to precisely determine the percentage of –NH_2 groups that is present on the coating surfaces after water immersion. Additionally, the coating surface morphology after water immersion will also be evaluated using scanning electron microscopy (SEM) imaging while the film thickness will be

determined using XPS in combination with C_{60} sputtering. After examining the chemical and structural characteristics of the PPFs after water immersion, cell studies will also be performed to evaluate the performance of the newly developed amino-rich PPFs in enhancing cell adhesion and proliferation.

2. Materials and methods

2.1. CPA-based PPF preparation

The plasma polymerisation set-up used to deposit CPA-based PPFs has already been described in detail in previous work and will therefore not be explained in this paper [29]. In this study, a small adaptation to the plasma set-up was however made – warping the high voltage wire with several additional layers of kapton tape – to minimize the possibility of generating a corona discharge around the high voltage wire. This small change to the plasma set-up has significantly improved the stability of the plasma discharge when using higher discharge powers of 15 and 20 W, which in turn yielded more consistent results. The plasma polymerization procedure applied was as follows: in a first step, the substrate (ultrahigh molecular weight polyethylene (UHMWPE) film with a thickness of 75 µm purchased from Goodfellow Cambridge UK) was fixed in the middle of the ceramic crucible covering the bottom plate electrode. In a next step, the stainless steel main plasma chamber was pumped down to a base pressure of 35 Pa using a rotary vane pump (Edwards-RV3). Argon gas was then introduced into the plasma chamber through the top mesh electrode at a rate of 4 standard litres per minute (slm) until a chamber pressure of 50 kPa was reached. At this chamber pressure, the argon flow rate was decreased to 0.4 slm after which the desired operating pressure of 50 kPa was stabilized by controlling a needle valve placed in front of the rotary vane pump. Subsequently, CPA vapour (Acros Organics, 98%) was added to the argon carrier gas after which the high voltage power source was switched on to start the PPF deposition on

the substrate. In this particular study, 3 different CPA flow rates (0.5, 0.25 and 0.125 g/h) were used in combination with applied discharge powers of 5, 10, 15 and 20 W resulting in W/FM values ranging from 36 to 576 MJ/kg as shown in Table 1. Afterwards, the as-deposited PPFs (denoted as BW: before water immersion) were subjected to different surface analysis tools, as will be described in detail in section 2.3.

Table 1. Overview of the applied plasma operational parameters and associated W/FM values for CPA-based PPF preparation.

CPA flow rate (g/h)	**Discharge power (W)**	**W/FM (MJ/kg)**
0.5	5	36
0.5	10	72
0.5	15	108
0.5	20	144
0.25	15	216
0.25	20	288
0.125	15	432
0.125	20	576

2.2. Water stability test

Immediately after preparation, some of the PPF samples were immersed in deionised water for 24 h before being subjected to various surface analysis techniques. Afterwards, the PPF samples were removed from the water, gently rinsed with some deionized water to remove any weakly bound residue and finally dried with compressed air. These PPF samples will be denoted as AW (after water immersion) in this particular paper.

2.3. Coating characterization

2.3.1. XPS

Surface chemical analysis of the coated samples before and after water immersion has been performed on a PHI Versaprobe II XPS spectrometer employing a monochromatic Al K_α

X-ray source (hν = 1486.6 eV) operating at 43.5 W. All measurements were conducted in a vacuum of at least 10^{-6} Pa and the photoelectrons were detected with a hemispherical analyser positioned at an angle of 45° with respect to the normal of the sample surface. Survey scans and individual high resolution spectra (C1s, O1s, and N1s) were recorded with a pass energy of 187.85 eV and 23.5 eV respectively. Elements present on the surfaces were identified from XPS survey scans, which have been performed on five different point locations per sample. The obtained elements were quantified with MultiPak software using a Shirley background and applying the relative sensitivity factors supplied by the manufacturer of the instrument. MultiPak software was also used to curve fit the high resolution C1s peaks. The hydrocarbon component of the C1s spectrum (285.0 eV) was used to calibrate the energy scale. In a next step, the peaks were deconvoluted using Gaussian–Lorentzian peak shapes and the full-width at half maximum (FWHM) of each line shape was constrained in the range 1.3-1.8 eV.

2.3.2. Chemical derivatization XPS

As mentioned above, curve fitting of the high resolution C1s peaks was performed in this work, however, in the case of CPA-based plasma polymers, where several nitrogen- and oxygen-containing groups were expected to be simultaneously present, a precise functional group identification/quantification was very difficult due to overlapping contributions in the high resolution C1s and N1s XPS spectra. For example, primary, secondary and tertiary amines are not readily distinguishable in high resolution C1s spectra, while a substantial overlap also occurs between C-N, C=N and C≡N groups in N1s spectra [30,31]. To overcome this difficulty, an advanced surface analysis technique combining XPS and chemical derivatization was used in this work to enable a meaningful quantification of the primary amine functional groups. For this purpose, CPA-based plasma deposits were first chemically derivatized by exposing the deposited coatings to TFBA vapour in a small glass chamber (pumped to a residual pressure of

1 kPa) at room temperature for 40 minutes. TFBA was chosen as derivatization molecule of interest since it is known to selectively react with $–NH_2$ groups, resulting in the incorporation of CF_3 groups on the deposits [32,33]. After derivatization, XPS survey scans were acquired on the derivatized samples using the same experimental XPS parameters as previously mentioned in section 2.3.1. After quantifying the obtained elements with Multipak software, the amino selectivity (NH_2/N) and the amino grafting efficiency (NH_2/C) of the deposits were determined [29].

2.3.3. XPS in combination with C_{60} sputtering

XPS as such only provides information on the chemical composition of the top layers of the fabricated PPFs as its analysis depth is typically smaller than 10 nm. To gather data on the chemical composition of the PPFs throughout their thickness, sputtering can be applied in combination with XPS analysis. In this work, a C_{60} primary ion beam was used to sputter the PPFs since it has demonstrated to produce significantly less accumulated material damage compared to sputtering with mono-atomic and atomic-cluster ion beams. The C_{60} ion source was operated at 10 kV and 20 nA. Sputtering of the PPFs was performed on a raster area of 4×4 mm^2 at an incident angle of 45°. Chemical depth profiling was carried out by performing XPS high resolution measurements of C1s, O1s and N1s regions after each 30 s sputter interval using 58.7 eV pass energy. This sequential sputtering-analysis route enabled the determination of the atomic concentration of C, N, and O throughout the total coating thickness. The number of sputter-analysis cycles was adapted for each particular sample so that the complete coating was removed and the substrate was reached.

2.3.4. ATR- FTIR

Besides standard XPS analysis, which provides chemical compositional information from the top nanometres from the CPA-based PPFs, FTIR was also used in this work to gather

more knowledge on the bulk chemical composition of the obtained plasma polymers as FTIR in combination with attenuated total reflection (ATR) is known to approximately analyse the top 0.6 µm of the PPFs [34]. FTIR spectra of the deposited BW and AW coatings were collected using a Bruker Tensor 27 spectrometer equipped with a single reflection ATR accessory (MIRacle®, Pike Technology) using a germanium crystal as internal reflection element. FTIR spectra were recorded in the wavenumber region 4500 to 700 cm^{-1} using a liquid nitrogen cooled MCT-detector with a resolution of 4 cm^{-1} and 64 scans were measured for each sample condition.

2.3.5. SEM imaging

The surface topography of the BW and AW deposits was visualized using a JEOL JSM-6010 PLUS/LV SEM device after gold sputtering the samples with a JEOL JFC-1300 Auto Coater for 25 s to enhance the sample conductivity. To obtain the SEM images shown in this work, an accelerating voltage varying from 5 to 20 kV using a filament temperature of 160°C was used.

2.4. Cell-coating interactions

2.4.1. Cell seeding

In a final step of this work, cells were seeded on the as-prepared PPF samples to examine their potential use in biomedical applications. For this purpose, the PPF samples were first sterilized by exposure to UV light for 30 min. Subsequently, human foreskin fibroblast (HFF) cells were seeded onto the PPFs in a 24-well plate at a density of 40,000 cells/100 µl of medium per sample followed by the addition of 400 µl additional medium after 4 h. Cell culture was performed using a DMEM (Dulbecco's Modified Eagle Medium) glutamax medium (Gibco Invitrogen) with 15% foetal calf serum (Gibco Invitrogen), 2 mM L-glutamine (Sigma-Aldrich), 10 U/ml penicillin, 10 mg/ml streptomycin and 100 mM sodium-pyruvate (all from

Gibco Invitrogen). In a next step, the cell cultures were incubated at 37°C under 5% CO_2 for 1 day (time required for HFFs to adhere on surfaces) after which cell viability and cell morphology was evaluated. HFFs seeded on tissue culture polystyrene (TCPS) were taken as a positive control.

2.4.2. Live/dead fluorescence microscopy

To qualitatively evaluate cell viability, PPFs seeded with HFFs were stained (life/dead staining) and subsequently visualized with a fluorescence microscope. 1 day after cell seeding, the supernatant was removed, the samples were rinsed twice and 1 ml of phosphate buffer saline (PBS) was added to the cultures. In a next step, the staining was performed by adding 2 µl (1 mg/ml) of calcein-acetylmethoxyester (Anaspec) supplemented with 2 µl (1mg/ml) propidium iodide (Sigma-Aldrich). Subsequently, the cultures were incubated for 10 min at room temperature in the dark, rinsed twice with PBS and were then visualized with a fluorescence microscope (Olympus IX 81) making use of appropriate filters.

2.4.3. MTT assay

A colorimetric MTT assay, using the yellow tetrazolium dye 3-(4, 5-dimethyldiazol-2-yl)-2, 5-diphenyltetrazolium bromide (MTT, Merck Promega), was performed to quantify cell viability by colorimetrically measuring the amount of metabolically active HFFs. The tetrazolium component is reduced in viable cells by mitochondrial dehydrogenase enzymes into blue-purple water-insoluble formazan, which can be solubilized by addition of lysis buffer and measured making use of spectrophotometry. For this purpose, the cell culture medium was first removed and replaced by 0.5 ml (0.5 mg/ml) MTT reagent. Subsequently, the cultures were incubated for 4 h at 37°C after which the MTT reagent was replaced by a lysis buffer (1% Triton-X100 in isopropanol/ 0.04 N HCl) to solubilize the water-insoluble formazan. The exposure to this lysis buffer was conducted for 30 min at 37°C. Afterwards, 200 µl of the

formazan solution was transferred to a 96-well plate and the absorbance of the coloured solution at 580 nm was measured using a spectrophotometer (Universal microplate reader EL 800, Biotek Instruments). The optical density of the coloured solution in this work was reported as a ratio compared to TCPS and triplicate measurements were performed at the same time point as the microscopic evaluation (1 day post cell seeding). For statistical analysis, one-way ANOVA was performed followed by a Tukey's HSD post hoc test and a P value <0.05 was considered to be significant.

2.4.4. Cell morphology evaluation

The morphology of the HFFs (shape of adhered cells and characteristics of lamellipodia and filopodia) adhering on the PPF samples was evaluated 1 day after cell seeding using SEM imaging. For this purpose, cell-seeded PPFs were gently removed from the culture medium and rinsed 3 times with PBS to remove non-adhered cells. Afterwards, the cells were fixed by soaking the samples in a fixing solution (2.5% glutaraldehyde in cacodylate buffer) at room temperature for 1 h. Afterwards, the samples were washed in the 0.1 M cacodylate buffer after which the cells seeded on the samples were dehydrated through immersion in increasing concentrations of ethanol (50%, 75%, 85%, 95% and 100%) for 10 min each. After the dehydration step, the samples were immersed in hexamethyldisilazane (HMDS) for 10 min, after which HMDS was refreshed and the samples were again immersed for 10 min. Subsequently, the samples were removed from HMDS and air-dried. The CPA-based PPFs covered by fixed dehydrated cells were subsequently coated with gold and viewed with SEM, according to the procedure described in section 2.3.5.

3. Results and discussion

3.1. XPS results

In a first step, the elemental composition of the as-deposited PPFs prepared with a deposition duration of 60 s was determined before and after water immersion using XPS survey scans. These XPS scans revealed that the CPA-based PPFs were only composed out of carbon, oxygen and nitrogen of which the relative concentrations were found to vary depending on the applied W/FM value.

Figure 1 (a) shows the evolution of the O/C ratio of the PPFs before and after water immersion (BW and AW). This figure clearly shows that in the region W/FM $\leq$ 144 MJ/kg the O/C ratio remains constant, while at W/FM $\geq$ 144 MJ/kg the O/C ratio gradually increases with increasing W/FM value. This observation for BW samples was already explained in previous work [29]: PPFs deposited at high energy input contain a higher amount of trapped free radicals because of a more intense fragmentation of the monomer. As a result, upon exposure to ambient atmosphere, more oxygen-based functionalities can be incorporated in these deposited plasma polymers [35,36]. A similar trend of the O/C ratio of the PPFs as a function of W/FM value could be noticed for AW samples, but for all W/FM values under study a considerably higher O/C ratio is found. For these samples, the additional oxygen incorporation is also more pronounced for the higher applied W/FM values. It can thus be concluded that water immersion results in an increase in the oxygen content of the CPA-based PPFs with the most pronounced increases at the highest W/FM values. This observation is in agreement with other literature available on amino-rich plasma polymerized coatings starting from the monomer allylamine, which also show an increase in oxygen content after immersion in water [30,36,37].

Figure 1 (b) shows the evolution of the N/C ratio as a function of applied W/FM values before and after water immersion (BW and AW) clearly showing a gradual enrichment in nitrogen content of the as-deposited PPFs with increasing W/FM value up to 288 MJ/kg, after which a constant N/C ratio is maintained as a function of W/FM value. Figure 1 (b) also reveals

that the N/C ratio of the PPFs decreases upon water immersion for all W/FM values under investigation with the most pronounced decreases in N/C ratio observed at the highest W/FM values. This nitrogen decrease is in excellent agreement with literature on allylamine-based plasma polymers, which also show a decrease in nitrogen amount upon water immersion [30,36,37]. The XPS survey scans thus clearly reveal that during immersion in water oxidation of the PPFs occurs in combination with a loss of nitrogen.

To determine the effect of water immersion on the amino grafting efficiency (NH_2/C) and amino grafting selectivity (NH_2/N), XPS survey scans have also been acquired for the TFBA-derivatized samples and Figure 1 (c) shows the evolution of the amino grafting efficiency as a function of W/FM before and after water immersion (BW and AW). An explanation for the particular behaviour of the NH_2/C ratio for as-deposited samples as a function of W/FM has already been given in previous work and will not be repeated here [29]. Figure 1 (c) reveals that there is a very strong decrease in NH_2/C ratio at W/FM values ≤ 72 MJ/kg suggesting a considerably loss of NH_2 groups on the surface of the PPFs prepared under these conditions upon water immersion. When the W/FM value is in the range 108-144 MJ/kg, the decrease in NH_2/C ratio is less distinct suggesting a larger retention of the amino groups on the surface of these PPFs after water immersion. However, at W/FM values above 144 MJ/kg, the decrease in NH_2/C ratio becomes again more pronounced suggesting poor stability of the amino groups upon water immersion on the PPFs prepared with high W/FM values. When observing the NH_2/C ratio of the AW PPFs as a function of W/FM value, the PPFs prepared at W/FM values ≤ 216 MJ/kg show a constant NH_2/C ratio of approximately 3%, while the PPFs obtained at W/FM values above 216 MJ/kg show a considerably lower NH_2/C ratio below 2%.

Figure 1 (d) shows the amino grafting selectivity as a function of applied W/FM value on the PPFs before and after water immersion (BW and AW). For a clear explanation of the

evolution of the NH_2/N ratio as a function of W/FM before water immersion, the reader is referred to previous work [29]. Upon water immersion, a similar trend as observed for the NH_2/C ratio can be seen: when comparing to the BW results, the NH_2/N ratio strongly decreases at W/FM values ≤ 72 MJ/kg, while in the range 108-144 MJ/kg, the decrease in NH_2/N ratio is rather small. However, a more pronounced decrease in NH_2/N ratio can again be observed at W/FM values above 144 MJ/kg. When observing the NH_2/N ratio of the AW PPFs as a function of W/FM value, the PPFs prepared at W/FM values ≤ 216 MJ/kg show a constant NH_2/N ratio of approximately 3%, while the PPFs obtained at W/FM values above 216 MJ/kg show a considerably lower NH_2/N ratio below 2%. The highest retention in amino functional groups upon water immersion is thus reached for the intermediate W/FM values, while high and low applied W/FM values result in less stable PPFs in terms of amino group retention.

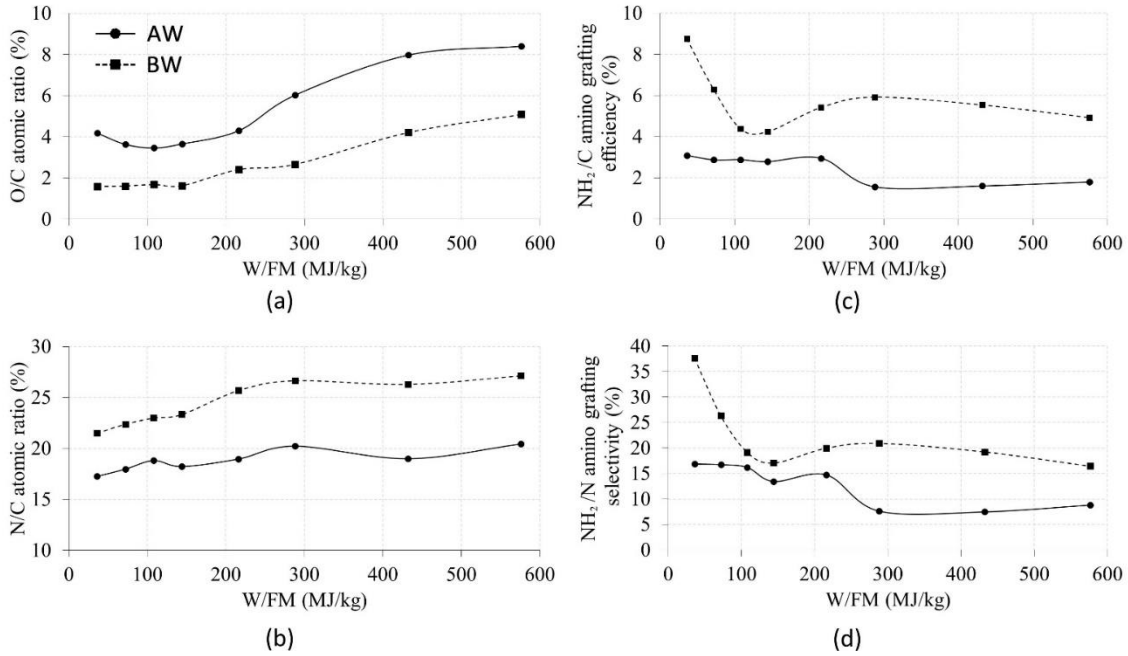

Figure 1. The evolution of the O/C ratio (a), N/C ratio (b), amino efficiency (c) and amino grafting selectivity (d) of the PPFs as a function of applied W/FM value before (BW) and after (AW) water immersion. The standard deviations on the depicted averaged values are < 2%.

Besides investigating XPS survey scans, curve fitting of high resolution C1s spectra was also performed in this work to extract additional information on the types of chemical

carbon bonds present at the surface of the PPFs before and after water immersion. The C1s peaks have been fitted making use of 4 distinct peaks: a component corresponding to C-C and C-H bonds at 285.0 eV, a peak at 285.9 eV which can be assigned to C-N groups (both primary, secondary and tertiary amines), a peak at 286.5 eV which can be assigned to C-O groups (alcohol or ether), as well as C≡N groups and/or C=N groups and finally a peak at 288.0 eV due to C=O (carbonyl) and/or N-C=O (amide) groups [29]. A typical fitted high resolution C1s peak can be seen in Figure 2, which shows the results of the PPF obtained at a W/FM value of 432 MJ/kg before and after water immersion. In this particular case, it can already be observed that the area of the peak at 286.5 eV considerably decreased upon water immersion, while the area of the other fitted components seems to be roughly unchanged. Water immersion thus mainly results in a loss of C-O and/or C≡N groups and/or C=N groups at the surface of the PPFs. Taking into account the observed decrease in N/C ratio and observed increase in O/C ratio upon water immersion, the loss of C≡N groups and/or C=N groups seems more likely to happen upon water immersion.

Based on the C1s curve fitting results, the relative concentrations of each functional group on the surface of the PPFs can also be determined and the results are presented in Figure 3 as a function of W/FM before and after water immersion. In this section, attention will only be given to the description of the effect of water immersion on the functional group concentration. For a detailed description of the functional group evolution as a function of W/FM on the as-deposited PPFs, the reader is referred to previous work [29]. In agreement with the conclusion drawn from Figure 2, it can be seen that the concentration of C-O/C=N/C≡N groups considerably decreases upon water immersion and this for all W/FM values under investigation. As previously mentioned, this decrease in mainly attributed to the loss of C=N/C≡N groups. At higher W/FM values, the loss of these carbon-nitrogen functional groups seems to be slightly more pronounced which is in agreement with the more pronounced

decrease in N/C ratio observed at higher W/FM values (Figure 1 (b)). Figure 3 also shows that upon water immersion, the relative concentrations of the peaks at 285.9 and 288.0 eV increase suggesting that water immersion results in a higher amount of C-N, C=O and/or N-C=O groups at the surface of the PPFs and this for all W/FM values under investigation. As Figure 1 shows that the amount of primary amines is decreasing upon water immersion, the increase in C-N concentration can thus only be attributed to an increase in secondary and tertiary amines as a result of water immersion. The decrease in concentration of the peak at 286.5 eV (C-O/C=N/C≡N) is also roughly equivalent to the total increase of the peaks at 285.9 eV (C-N) and 288 eV (C=O/N-C=O). It can thus be hypothesized that upon water immersion hydrolysis of the primary amine groups and C=N/C≡N groups occurs resulting in the formation of other functional groups including secondary/tertiary amines, amides, carbonyls and alcohols/ethers. To conclude, it can thus be stated that water immersion results in a loss of C-NH_2, C=N and C≡N groups and the simultaneous incorporation of oxygen at the surface as amides, carbonyls and alcohols/ethers. As no peaks above 288 eV are seen in the high resolution C1s peaks of the PPFs before and after water immersion, the presence of COOH groups at the surface of the PPFs can also be eliminated.

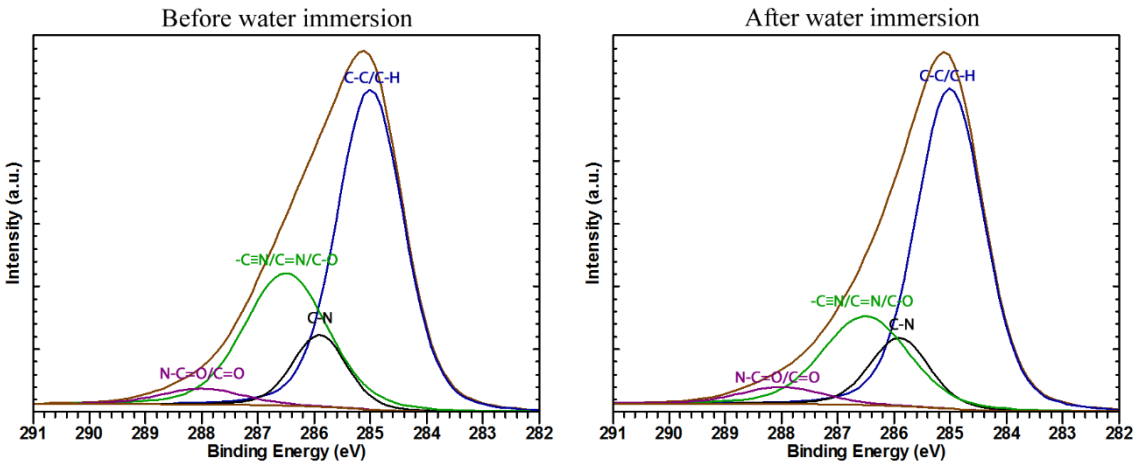

Figure 2. Deconvolution of the high resolution C1s spectra of the PPF obtained at a W/FM value of 432 MJ/kg before and after water immersion.

The results mentioned above provide interesting information on the changes in the top surface chemical composition of the PPFs upon water immersion. Unfortunately, since XPS has an analysis depth < 10 nm, it is however very difficult to draw conclusions on the PPF stability in water based on these XPS results. Furthermore, it has already been shown in literature that regardless of the stability of the PPF in an aqueous environment, it will anyhow experience an initial loss in amino groups due to the extraction of soluble low molecular weight oligomers (LMWO) [38,39]. To have a better understanding of how water influences the PPF bulk properties, further analysis using FTIR and C_{60}-sputtering in combination with XPS was also performed in this work, of which the results will be presented below. As mentioned in sections 2.3.3 and 2.3.4, the first technique has a higher analysing depth of approximately 600 nm while the second method allows obtaining the chemical composition throughout the total thickness of the PPFs.

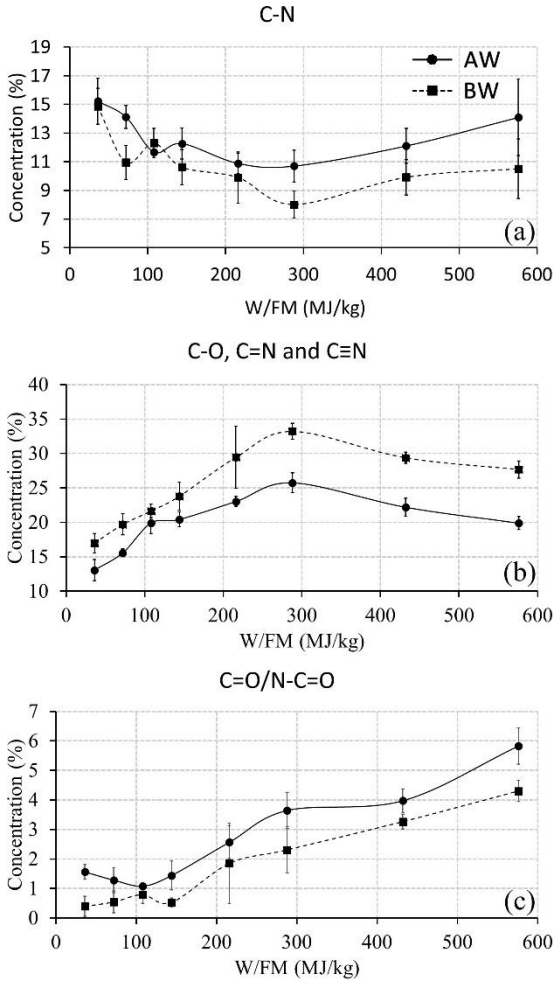

Figure 3. Relative concentrations of the peaks at 285.9 eV (C-N groups) (a), 286.5 eV (C-O, C=N and C≡N groups) (b) and 288.0 eV (C=O and/or N-C=O groups) (c) as a function of W/FM value before and after water immersion.

3.2. FTIR results

Figure 4 shows the FTIR spectra of PPF samples that were prepared using the same plasma conditions as for XPS analysis both before and after being immersed in water for 24 h. The characteristic peaks of the CPA-based PPFs prior to water immersion have already been thoroughly described in previous work and are for sake of clarity summarized in Table 2 [29,40].

Table 2. Assignment of the FTIR peaks observed for the CPA-based PPFs.

Wavenumber (cm^{-1})	Assignment	Functional class
3600-3200	N-H stretching	amines/amides
3600-3200	O-H stretching	alcohols/carboxylic acids
3000-2850	C-H stretching	alkanes
2200-2100	C≡N stretching	(iso)nitriles
1690-1630	C=O stretching	amides
1690-1640	C=N stretching	imines
1670-1550	N-H deformation	amines
1640-1550	N-H deformation C-N stretching	amides
1460	C-H deformation	alkanes
1380	C-H deformation	alkanes
1170-1050	C-N stretching	amines
1260-1000	C-O stretching	alcohols/ethers

The FTIR spectra shown in Figure 4 as a function of W/FM value thus confirm the obtained XPS results as they also reveal the presence of amines (C-N), amides (N-C=O) and imines (C=N) on the PPFs prior to water immersion. Since there are no peaks in the wavenumber range 1900-1700 cm^{-1}, it can be concluded that carbonyl or carboxylic groups are not present in the PPFs. This result in combination with the previously gathered XPS data implies that the oxygen content in the PPFs is mainly attributed to the presence of C-O-C, N-C=O and C-OH functional groups. Unfortunately, the peaks of O-H stretching (3600-3200 cm^{-1}) and C-O stretching (1260-1000 cm^{-1}) are also overlapping with the N-H stretching (3600-3200 cm^{-1}) and C-N stretching (1170-1050 cm^{-1}) bands respectively. Consequently, it is impossible to confirm the presence of C-O-C and C-OH functional groups in the coatings from the gathered FTIR spectra. Nevertheless, as there is a small oxygen concentration present at the surface of the PPFs prior to water immersion (see Figure 1 (a)), it is anticipated that C-O-C, C-OH and N-C=O functional groups are present in the PPFs, but in low concentrations.

The FTIR spectra depicted in Figure 4 also reveal that the characteristic peak of (iso)nitriles in the region 2400-2050 cm^{-1} is present for all PPFs under study except for the PPF prepared at 36 MJ/kg. This result is in disagreement with previously gathered FTIR spectra, in which (iso)nitriles were only observed at the highest applied W/FM value (576 MJ/kg) [29]. This discrepancy can be explained by the small changes made to the DBD reactor which improved the stability of the discharge, which could in turn affect the final chemical composition of the PPFs. The presence of (iso)nitriles is consistent with literature as it has already been observed that CPA-based PPFs contain a significant amount of C≡N groups [30]. Moreover, in a recent study, it was also found that CPA was more prone to undergo dehydrogenation when compared to allylamine resulting in a higher concentration of C≡N groups during plasma polymerisation [41]. The FTIR spectra of Figure 4 also reveal that the intensity of the broad C≡N band increases with increasing W/FM value in the range 72 to 288 MJ/kg after which the intensity rapidly decreases at higher W/FM values of 432 and 576 MJ/kg. A similar trend with varying W/FM value has also been found in the evolution of the peak area at 286.5 eV (Figure 3 (b)), which could be allocated to a combination of C-O, C=N and C≡N groups. From the additional FTIR spectra, it can thus be concluded that among these functional groups, the amount of C≡N groups present in the PPFs is affected by the applied W/FM value.

After water immersion, significant changes can be seen in the FTIR spectra of the PPFs. At W/FM values ≤ 288 MJ/kg, a significant decrease in peak intensity in the region 3500-3100 cm^{-1} (OH and NH stretching) can be seen after water immersion. Additionally, also the broad peak in the region 1750-1500 cm^{-1} (amide/amine N-H deformation, C=N stretching and C-N stretching of amides) strongly decreases upon water immersion, while the C≡N peak in the region 2400-2050 cm^{-1} completely disappears. Finally, also the intensity of the broad peak in the region 1250-1050 cm^{-1} decreases (C-N stretching) upon water immersion. These above-mentioned changes thus suggest a loss of C-N, C≡N and C=N functional groups upon water

immersion, which is in disagreement with the obtained XPS results, where only a loss in C≡N and C=N functional groups and a shift of primary to secondary/tertiary amines was found. However, it should be kept in mind that a change in thickness of the deposited coatings may occur after water immersion. Consequently, this might influence the intensity of obtained FTIR peaks for PPFs that were submerged into water. Upon closer inspection, the FTIR spectra of PPFs prepared with W/FM values ≤ 288 MJ/kg also show a broadening of the peak in the region 1200-1000 cm^{-1} which could indicate the incorporation of C-OH or C-O-C functional groups resulting from the oxidation of trapped free radicals in the PPFs during water immersion [36]. This observation is also in agreement with the previously obtained XPS results, which revealed an increase in O/C ratio upon water immersion. By combining both XPS and FTIR results, it can be concluded that at W/FM values ≤ 288 MJ/kg, water immersion results in a significant loss in C=N/C≡N groups and a shift of primary to secondary/tertiary amines combined with the incorporation of oxygen at the surface as amides and alcohols/ethers.

In case of W/FM values above 288 MJ/kg, the FTIR spectra after water immersion show no peaks characteristic for the PPFs anymore as only the peaks attributed to the UHMWPE substrate can be seen. These results thus suggest that either these coatings are almost completely dissolved during water immersion, which seems to be highly unlikely taking into account the expected higher cross-linking degree of the coatings at higher W/FM values. Therefore, it is more likely that the coatings delaminate from the substrate during water immersion. Despite the delamination of the coatings at high W/FM values after water immersion, a very thin coating layer however remains on top of the UHMWPE substrate, as evidenced from the XPS results previously shown in this work. In order to confirm the hypothesis about the coating delamination, additional analyses are performed making use of XPS combined with C_{60} sputtering and SEM and will be discussed in the next sections.

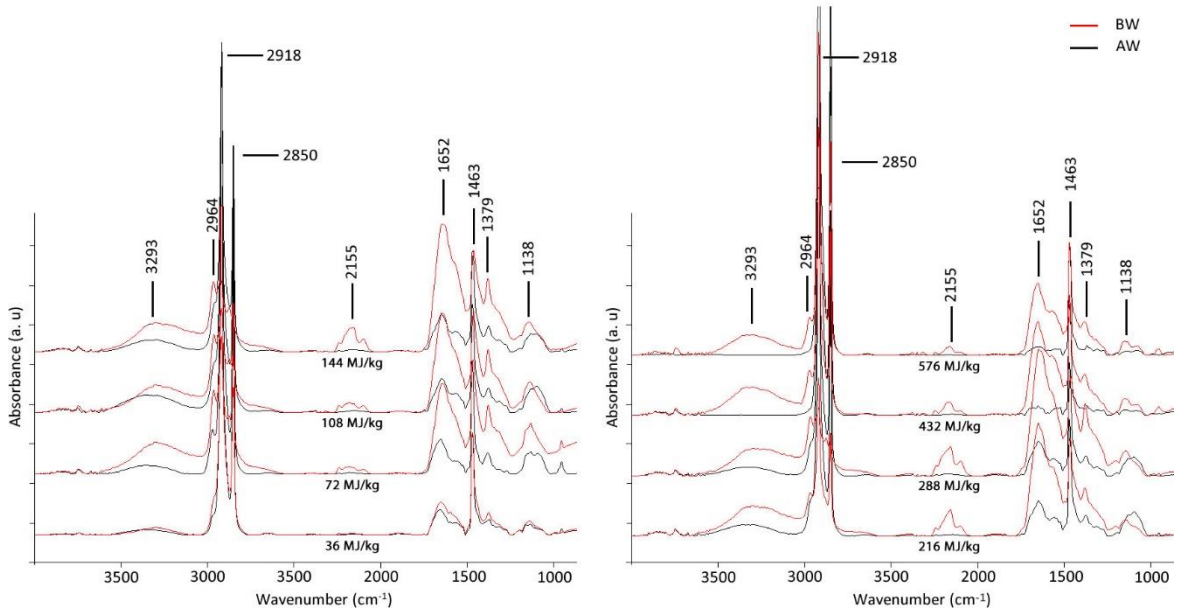

Figure 4. FTIR spectra of CPA-based PPFs prepared at different W/FM values (36 – 576 MJ/kg) before and after water immersion (BW and AW).

3.3. XPS sputter depth profiling

As mentioned above, C_{60} ion bombardment in combination with XPS analysis was performed to complement the FTIR results and to demonstrate the chemical composition distribution along the thickness of the PPFs. Taking into account all the results obtained before, the deposits prepared at 216 and 432 MJ/kg were used for comparison. These conditions were selected as examples of coatings that are suspected to undergo dissolving and delamination upon immersion in water respectively. To have a fair comparison between the depth profiles of these selected samples, the film thickness was fixed at approximately 600 nm for both conditions by varying the deposition time. Figure 5 shows the XPS depth profiles of the selected samples using C_{60} ion beam sputtering before (BW) and after (AW) the water stability test. As expected, the in-depth distribution of the samples demonstrates the presence of C, N and O elements at the beginning of the sputtering procedure, which is consistent with the previously obtained XPS results at the top surface of the PPFs. Moreover, the O/C and N/C ratios at the top surface in Figure 5 (a) and (b) are the same as the ones reported above in Figure 1 (a) and (b) respectively. Figure 5 also reveals a constant nitrogen and oxygen concentration

through the coating thickness for the freshly prepared samples suggesting an excellent in-depth homogeneity of the PPFs. After a sputter time of approximately 20 minutes, the carbon content however starts to increase for both samples while the nitrogen content decreases suggesting that the UHMWPE substrate is almost reached.

From Figure 5 (c) and (d), it is also clear that, after the water immersion step, the time needed for a complete film sputtering is much shorter in comparison to freshly prepared samples. More specifically, the time needed for a complete sputtering of the coating prepared at 216 MJ/kg after water immersion is more than two times shorter than in case of the original deposit suggesting a significant loss of the coating thickness during water immersion. Moreover, also the nitrogen content at the top surface and inside the bulk is lower when compared to the as-prepared 216 MJ/kg PPF. In contrast, the oxygen content at the top surface increases upon water immersion, which is consistent with the XPS results shown in Figure 1 (a). However, this increased oxygen content is mainly present at the top coating surface as the oxygen concentration rapidly decreases with increasing sputter time. From these XPS sputter results, it can thus be confidently declared that the coating prepared at 216 MJ/kg is partly dissolved during water immersion. Moreover, oxidation also occurs at the top coating surface due to direct contact with water molecules and insufficiently cross-linked nitrogen-containing functional groups dissolve from the surface and the bulk of the PPF as the amount of detected nitrogen stays constant through the coating thickness.

In contrast to the PPF prepared at 216 MJ/kg, the XPS depth profile of the PPF prepared at 432 MJ/kg after water immersion as depicted in Figure 5 (d) shows a complete sputtering of the coating after a sputter time of only 1 min. This result suggests that the coating was no longer present at the UHMWPE substrate and that it most likely delaminated from the substrate during water immersion, which is consistent with the obtained FTIR spectra. Nevertheless, Figure 5

(d) also reveals that a very thin coating layer does remain on top of the substrate as a few sputtering cycles were required to obtain absence of the N1s signal from the deposit. This result is in agreement with the XPS results obtained in section 3.1, where oxygen and nitrogen was still detected on the PPF prepared at 432 MJ/kg upon water immersion. Similar as in case of the 216 MJ/kg sample, the remaining very thin coating contains a higher amount of oxygen at the top surface and a lower amount of nitrogen compared to the freshly prepared sample.

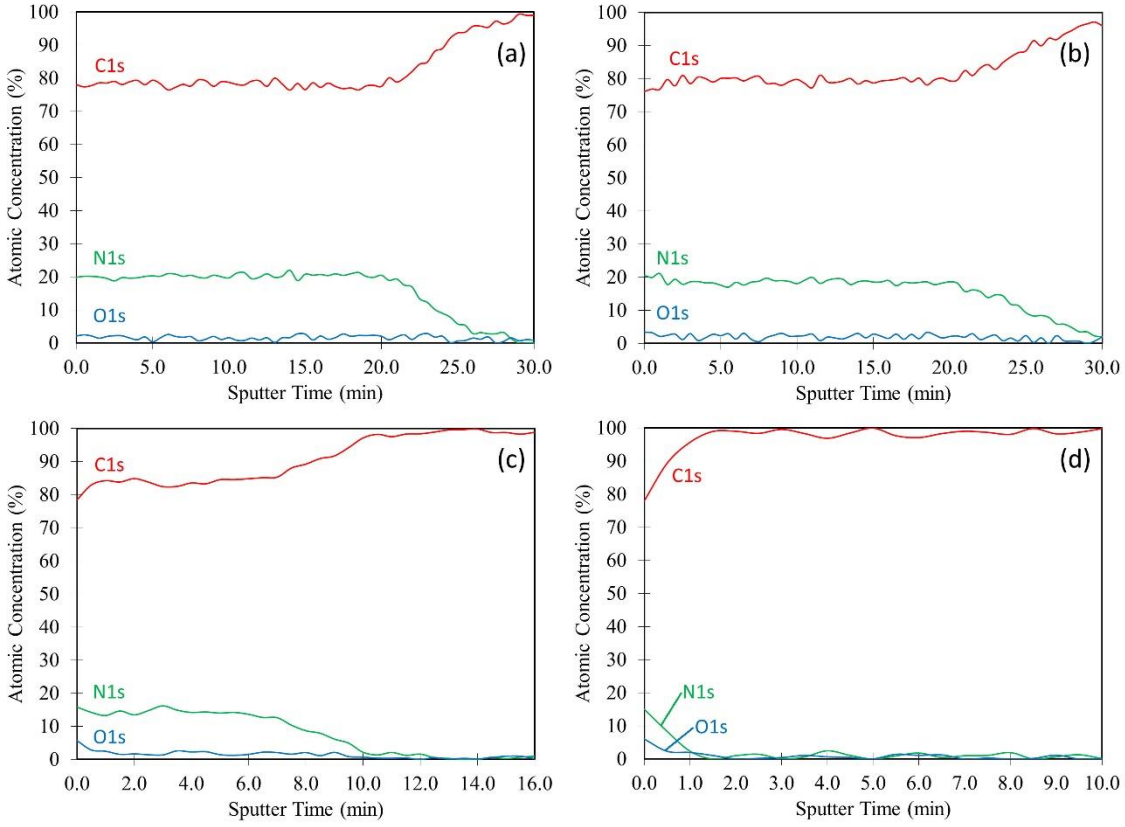

Figure 5. C_{60} sputter depth profiles of PPFs prepared at 216 and 432 MJ/kg before (a, b) and after (c, d) water immersion.

3.4. SEM imaging

To further reinforce the hypothesis of coating delamination at higher W/FM values, SEM imaging was also used to investigate the surface morphology of the PPFs. For this purpose, PPFs were prepared using the same experimental conditions as in case of C_{60}-sputtering and these samples were examined with SEM before and after water immersion of which the results are shown in Figure 6. It can be clearly seen that the deposition of the PPFs

greatly altered the surface morphology of the original UHMWPE substrate when comparing the SEM images of Figure 6 (b) and (c) to Figure 6 (a). The surface morphology between the 216 and 432 MJ/kg PPFs is also very different from each other apart from being free from pinholes. The most prominent distinction between Figure 6 (b) and (c) is the presence of cracks stretching all across the entire substrate surface on the latter image, while small particles are scattered across the surface of the PPF prepared at 216 MJ/kg. In general, the coating morphology in Figure 6 (b) is more uniform and the coating has a rougher topography than the surface of the PPF prepared at 432 MJ/kg. It is also important to mention that with the selected film thickness of 600 nm for both PPFs, all surface morphological features of the underlying UHMWPE substrate are no longer visible.

After water immersion, the UHMWPE substrate remains exactly as it was before water immersion as to be expected (see Figure 6 (d)). However, the surface morphology of both PPFs significantly changes after the water stability test. Figure 6 (e) reveals a significant degradation of the coating prepared at 216 MJ/kg with small cracks present across the entire coating surface. Nonetheless, this SEM image still proves the presence of the PPF on the substrate after water immersion. On the other hand, the SEM image of the PPF prepared at 432 MJ/kg after water immersion appears to look almost identical to the pristine UHMWPE substrate as only a thin layer of PPF that is barely noticeable in Figure 6 (f) is remaining as tiny folds scattered throughout the image area. This thin layer is however more apparent on the SEM image obtained during the cell-coating interaction studies performed in the next section (Figure 7 (c2)). The SEM images shown in this section thus confirm the previously obtained results: upon water immersion, the PPF prepared at 216 MJ/kg partly dissolves, while the PPF prepared at 432 MJ/kg delaminates from the UHMWPE substrate.

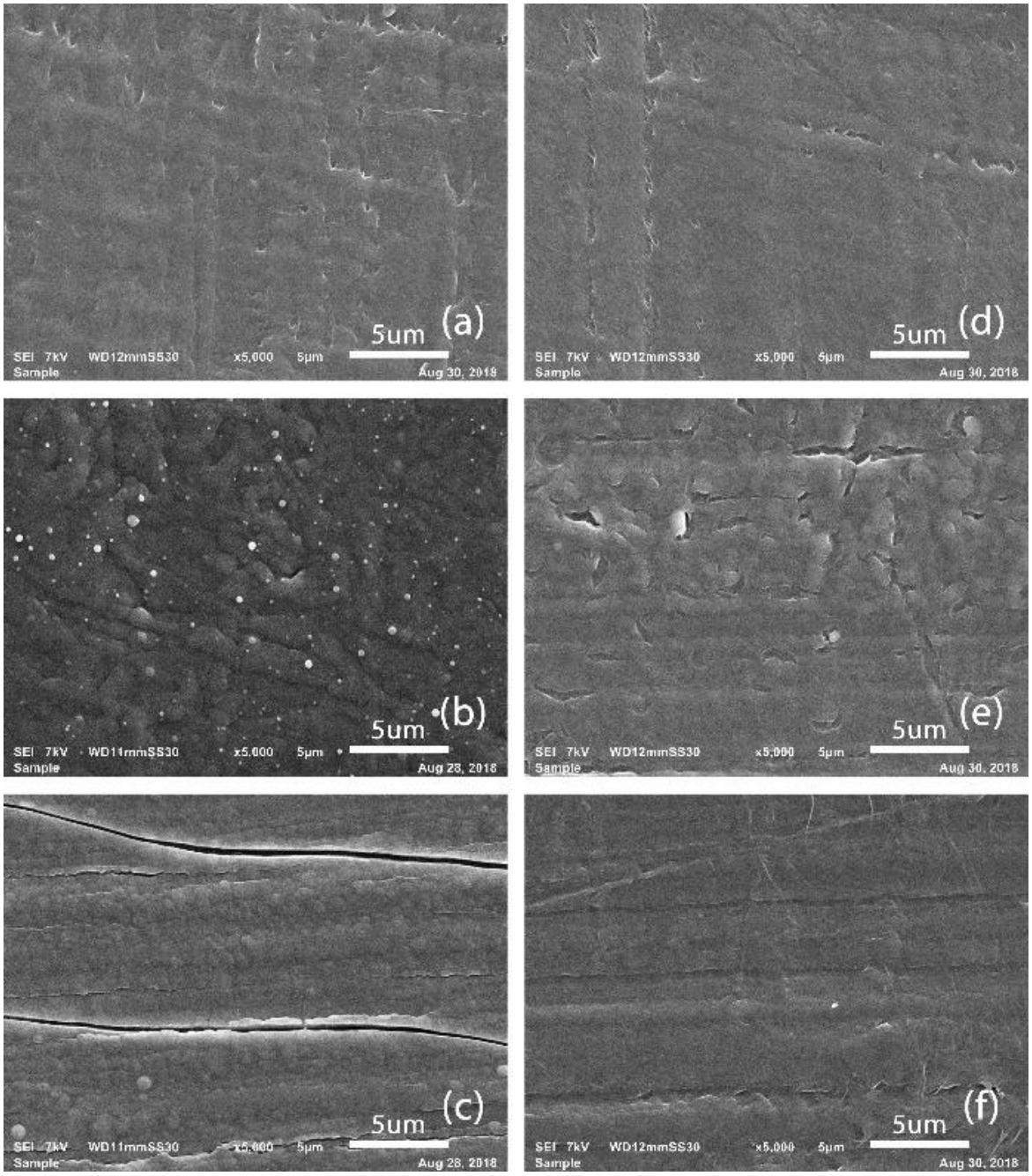

Figure 6. SEM images of untreated UHMWPE (a) and PPFs prepared at 216 MJ/kg (b) and 432 MJ/kg (c) with a thickness of 600 nm before water immersion and SEM images of untreated UHMWPE (d) and PPFs prepared at 216 MJ/kg (e) and 432 MJ/kg (f) with a thickness of 600 nm after water immersion.

By combining the observations from SEM, FTIR and XPS depth profiling, it is evident that the PPFs under investigation in this study are not stable in water and their degradation behaviour is affected by the W/FM value applied during plasma polymerization. The FTIR and C_{60} sputtering results show that the coatings prepared at 216 MJ/kg are gradually dissolving

when being immersed in water and this dissolving step most likely also occurs for the PPFs prepared at lower W/FM values as even lower discharge powers are applied under these conditions. Furthermore, the reduction of the nitrogen content detected with XPS analysis upon water immersion indicates a significant amount of nitrogen-containing LMWO in the bulk of the freshly prepared films at W/FM values which can easily diffuse from the coating bulk into the water. The poor stability of the PPFs prepared at W/FM values ≤ 216 MJ/kg can be explained by the insufficient discharge power used during coating deposition which typically results in a low cross-linking degree within the PPF structures [14,42,43].

For the PPF prepared at 432 MJ/kg, the XPS depth profile demonstrates a complete coating removal after a few sputtering cycles. This observation together with SEM imaging and FTIR results where a thin layer of PPF can be barely seen on the UHMWPE substrate and a complete loss of the peaks that are characteristic for the PPF prepared at 432 MJ/kg all suggest film delamination after water immersion. This peculiar outcome can be explained by the following findings in literature: First of all, it has been shown that the intrinsic stress within the bulk of a thick, highly cross-linked PPF is significantly higher than in case of a less-crosslinked, thinner coating [44,45]. This stress on the top coating surface typically causes crack formation in the freshly deposited PPFs, which is also observed for the PPF prepared at 432 MJ/kg (see Figure 6 (c)). Subsequently, upon contact with an aqueous environment, such a cracked coating surface will experience two important events [46]. First, bending and curling of the top coating layer will occur due to the previously mentioned intrinsic stress when placed in water. Secondly, due to the presence of cracks on the coating surface, water can easily penetrate inside the deposit and even in between the PPF and the substrate. The combination of these two factors will facilitate the delamination of the coating from the substrate, which was indeed observed for the sample prepared at 432 MJ/kg in this study. Taking into account the obtained FTIR spectra, it is hypothesized that coating delamination also occurs for the PPF

prepared at 576 MJ/kg. To conclude, it can thus be stated that the PPFs prepared at W/FM values ≥ 432 MJ/kg delaminate from the substrate as a result of their high cross-linking degree.

3.5. Cell-coating interactions

After the extended surface characterization of the PPFs in the previous sections, the cell-coating interactions are investigated in this part of the study as the developed coatings are particularly interesting for cell growth. To evaluate the cytotoxicity behaviour of the PPFs prepared at 216 and 432 MJ/kg, the adhesion and viability of HFF cells on the coatings were evaluated 24 h post seeding. Similar as in case of XPS depth profiling and SEM imaging, the film thickness was fixed at 600 nm for both PPFs under study. Figure 7 shows the fluorescence and SEM images of the cells seeded on untreated UHMWPE and on the PPFs prepared at 216 and 432 MJ/kg. As expected, the fluorescence and SEM images depicted in Figure 7 (a1) and (a2) respectively show that on the UHMWPE substrate the cells possess a round shape and also appear to be poorly attached to the substrate. These observations are due to the lack of surface functionalities which fail to elucidate the adsorption of proteins encouraging cell adhesion. In contrast, the fluorescence images of the PPFs prepared at 216 and 432 MJ/kg shown in Figure 7 (b1) and (c1) reveal that a significantly higher number of cells attach to the surface of the remaining coating while these cells also exhibit a more spread morphology. When comparing both PPFs, the cell density appears to be slightly higher for the coating prepared at 216 MJ/kg, however, at the same time, also a higher number of dead cells is present. Although the cell density for the PPF prepared at 432 MJ/kg is lower, there are however more cells with a spread out and elongated morphology on the surface of this coating, which is a good indication for the healthy growth of the fibroblasts. Further evidence of the improvement in cell-surface interactions on both PPFs can be found in the SEM images shown in Figure 7 (b2) and (c2). These images clearly show the formation of lamellipodea and filopodia sprouting from the

cells. This spread-out cell morphology is a clear sign of the initial process of the anchoring of the cells to the surfaces [46]. The images depicted in Figure 7 thus clearly illustrate that the deposition of the PPFs on the UHMWPE substrate considerably increases cell adhesion.

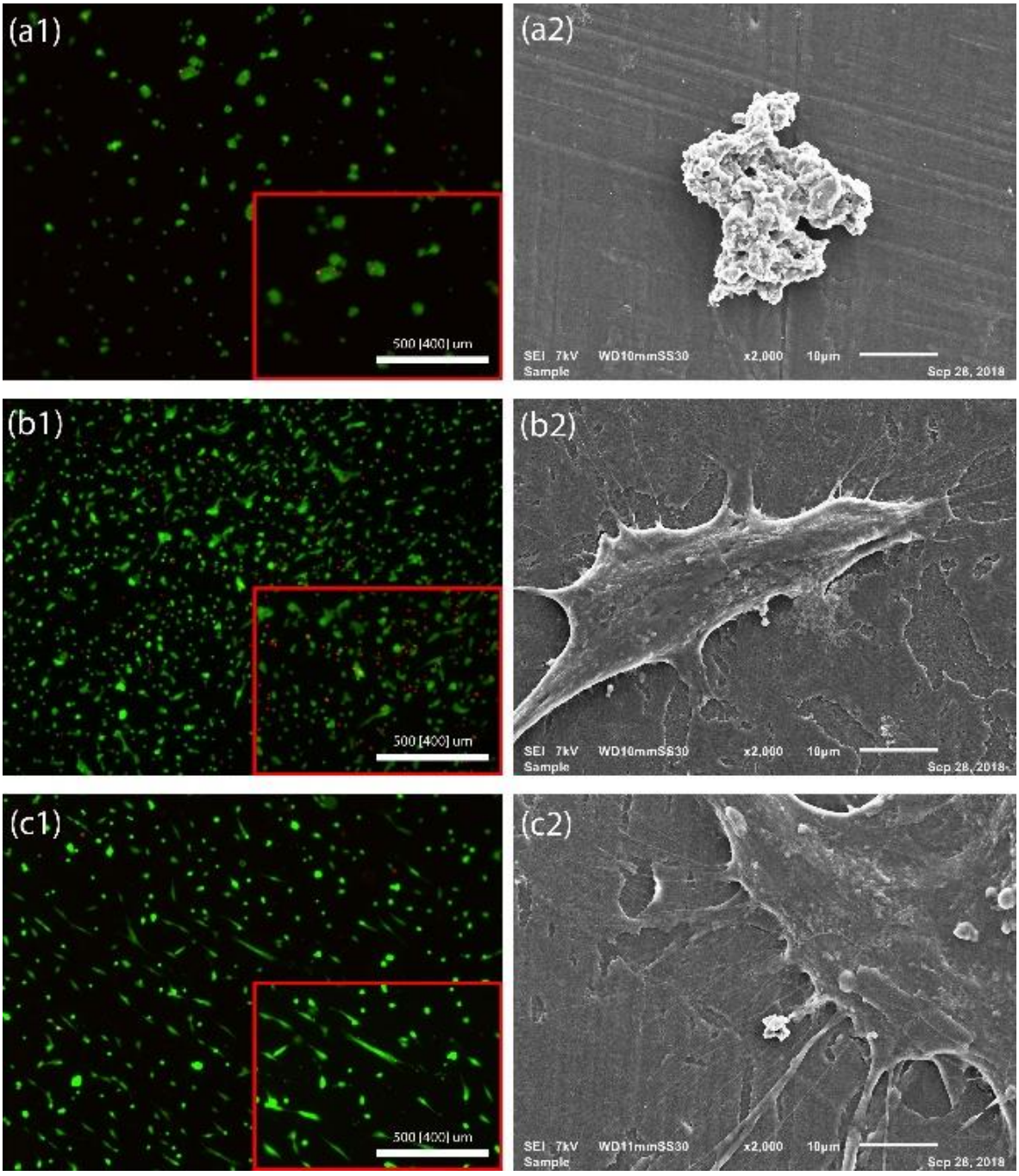

Figure 7. Fluorescence (1) and SEM (2) images of HFFs adhering on (a) untreated UHMWPE, (b) the PPF prepared at 216 MJ/kg and (c) the PPF prepared at 432 MJ/kg.

To quantify the viability of the cells, an MTT assay is also performed 1 day after cell seeding and the outcome of this assay is summarized in Figure 8. This figure clearly shows that

the cell viability is 2 to 3 times larger on the PPFs than on the untreated sample, which is clearly due to the higher number of adhered cells on these PPFs. Interestingly, although the fluorescence image of the sample prepared at 216 MJ/kg shows a higher cell density compared to the PPF prepared at 432 MJ/kg, the MTT results show otherwise as the PPF prepared at 432 MJ/kg has a roughly 10% higher cell viability. This higher cell viability can however be explained by the fact that the cells on the 432 MJ/kg sample possess a higher mitochondrial activity, as evidenced by the higher number of cells having a spread morphology. As a consequence, there is a higher reduction rate of MTT into formazan which in turn significantly increases the optical density of the solution [47–49]. The cell studies performed in this section thus provide strong evidence for the enhanced cell-surface interactions on the PPFs prepared at 216 and 432 MJ/kg. From this, it can be concluded that the coating remaining on top of the substrate after immersion in cell culture medium, which is very thin in case of the 432 MJ/kg sample due to delamination of the coating, is sufficient to provide excellent cell attachment onto the UHMWPE substrate. Moreover, the dissolution of the coating at 216 MJ/kg in the cell culture medium is also not causing cytotoxic effects. Nevertheless, efforts should be undertaken in the near future to avoid delamination of the PPFs prepared at high W/FM values from the substrate.

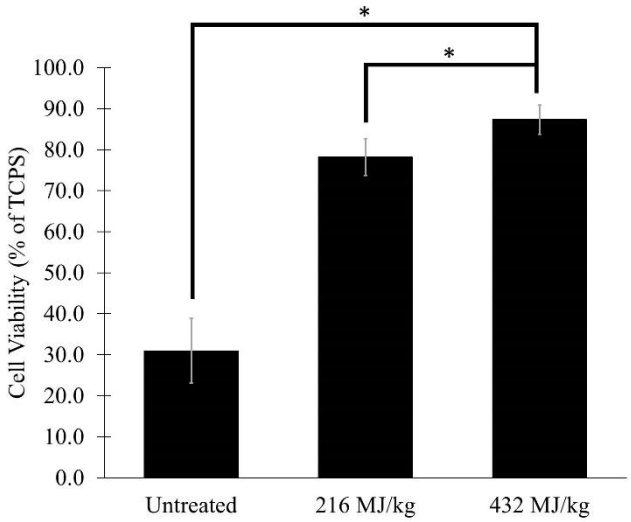

Figure 8. MTT assay results 1 day after cell seeding on untreated UHMWPE and on the PPFs prepared at 216 and 432 MJ/kg. (denotes statistical significance at P<0.05)*

4. Conclusions

In this study, the stability of CPA-based PPFs in water has been investigated by means of XPS, FTIR, SEM imaging and XPS chemical depth profiling using C_{60} sputtering. By comparing the XPS results obtained for the coatings before and after immersion in water for 24 h, it was possible to conclude that a thin coating layer remained on the UHMWPE substrate after the water stability test. Moreover, XPS and FTIR results also revealed a decrease in the nitrogen content and an increase in the oxygen content of the coatings after water immersion. These changes in chemical composition were caused by a significant loss in C=N/C≡N groups and a shift of primary to secondary/tertiary amines combined with the incorporation of oxygen at the surface as amides and alcohols/ethers. The XPS results also showed that there was no direct correlation between the applied W/FM value and the observed decreases in NH_2/C and NH_2/N ratios. The FTIR spectra of the CPA films prepared at W/FM values ≤ 288 MJ/kg still contained absorption peaks specifically for this type of PPF and thus confirmed the presence of a considerably thick coating on the substrate after the water stability test. However, these

characteristic absorption peaks were no longer found in the FTIR spectra obtained after water immersion for the samples prepared at 432 and 576 MJ/kg. Based on these FTIR results, a hypothesis was proposed: the PPF partly dissolved at low applied W/FM values, while the coating delaminated from the substrate at high applied W/FM values. This hypothesis was confirmed by a further coating analysis using XPS chemical depth profiling by means of C_{60} sputtering and SEM imaging. Indeed, the C_{60} sputter profiles obtained for the coating prepared at 216 MJ/kg demonstrated the presence of a thinner CPA film with a lower nitrogen content on the UHMWPE substrate after water immersion in comparison to the freshly deposited coating. In contrast, after water immersion of the PPF prepared at 432 MJ/kg, only a very thin coating layer (most likely of the order of a few nanometres) remained on the substrate as complete sputtering of this particular coating only required a few sputter cycles. These chemical depth profiling results thus support the hypothesis that CPA-PPFs prepared at W/FM values $\leq$ 288 MJ/kg experience partial dissolution in an aqueous environment due to the insufficient discharge power used during deposition. On the other hand, the PPFs prepared at W/FM values above 288 MJ/kg undergo delamination during water immersion due to bending and curling of the edges of cracks which occur due to the accumulation of intrinsic stress on the top coating layer of the freshly prepared samples as has been reported before in literature. In addition, water easily penetrates in the films via these cracks, thereby further facilitating delamination. Nevertheless, a very thin layer of these coatings still remains on the substrate after water immersion as also evidenced from SEM imaging. Despite the rather poor stability of the PPFs under study in this work, they still show an excellent adhesion of fibroblasts with a substantially higher cell density on the PPFs compared to the bare substrate. Consequently, coating dissolution or delamination was not causing any cytotoxicity. Nevertheless, in the near future, efforts will be undertaken to avoid the delamination of the CPA-PPFs prepared ad high W/FM values from the substrate during water immersion.

Acknowledgments

This research has received funding from the European Research Council (ERC) under the European Union's Seventh Framework Program (FP2007-2013): ERC Grant Agreement number 335929 (PLASMATS). The authors also acknowledge the support of the Research Foundation Flanders (FWO) for financing the Buckminster fullerene ion gun (Medium sized research infrastructure AUGE/15/04) for advanced XPS chemical depth profiling of polymer materials.

Reference

[1] N. a. Bullett, D.P. Bullett, F.-E. Truica-Marasescu, S. Lerouge, F. Mwale, M.R. Wertheimer, Polymer surface micropatterning by plasma and VUV-photochemical modification for controlled cell culture, Appl. Surf. Sci. 235 (2004) 395–405. doi:10.1016/j.apsusc.2004.02.058.

[2] F.P.S. Guastaldi, D. Yoo, C. Marin, R. Jimbo, N. Tovar, D. Zanetta-Barbosa, P.G. Coelho, Plasma treatment maintains surface energy of the implant surface and enhances osseointegration, Int. J. Biomater. (2013) ID 354126. doi:10.1155/2013/354125.

[3] E.D. Yildirim, D. Pappas, S. Güçeri, W. Sun, Enhanced cellular functions on polycaprolactone tissue scaffolds by O2 plasma surface modification, Plasma Process. Polym. 8 (2011) 256–267. doi:10.1002/ppap.201000009.

[4] Q. Chen, R. Forch, W. Knoll, Characterization of Pulsed Plasma Polymerization Allylamine as an Adhesion Layer for DNA Adsorption / Hybridization, Chem. Mater. 16 (2004) 614–620.

[5] D. Cossement, L. Denis, D. Cossement, T. Godfroid, F. Renaux, C. Bittencourt, R. Snyders, M. Hecq, Synthesis of Allylamine Plasma Polymer Films : Correlation between Plasma Diagnostic and Film Characteristics Synthesis of Allylamine Plasma Polymer Films : Correlation between Plasma Diagnostic and Film Characteristics, Plasma Process. Polym. 6 (2009) 199–208. doi:10.1002/ppap.200800137.

[6] H. Dave, L. Ledwani, N. Chandwani, B. Desai, S.K. Nema, Surface activation of polyester fabric using ammonia dielectric barrier discharge and improvement in colour depth, 39 (2014) 274–281.

[7] M. Okamoto, R. Yakawa, M. Wakasa, T. Wakisaka, Functional-group analysis on a polymer surface by X-ray photoelectron spectroscopy preceded by selective chemical derivatization, BUNSEKI KAGAKU. 47 (1998) 261–265. http://apps.webofknowledge.com/full_record.do?product=UA&search_mode=GeneralSearch&qid=7&SID=T1wxkUDdbbbaOWzrXc8&page=1&doc=2 (accessed May 6, 2015).

[8] D. Yan, J. Jones, X.Y. Yuan, X.H. Xu, J. Sheng, J.C.-M. Lee, G.Q. Ma, Q.S. Yu,

Plasma treatment of electrospun PCL random nanofiber meshes (NFMs) for biological property improvement., J. Biomed. Mater. Res. A. 101 (2013) 963–72. doi:10.1002/jbm.a.34398.

[9] A. Hadjizadeh, C.J. Doillon, Endothelial cell behaviour on gas-plasma-treated PLA surfaces: the roles of surface chemistry and roughness, J. Tissue Eng. Regen. Med. 4 (2010) 524–531. doi:10.1002/term.

[10] A. Bourkoula, V. Constantoudis, D. Kontziampasis, P.S. Petrou, S.E. Kakabakos, A. Tserepi, E. Gogolides, Roughness threshold for cell attachment and proliferation on plasma micro-nanotextured polymeric surfaces: the case of primary human skin fibroblasts and mouse immortalized 3T3 fibroblasts, J. Phys. D. Appl. Phys. 49 (2016) 304002. doi:10.1088/0022-3727/49/30/304002.

[11] T. Saito, H. Hayashi, T. Kameyama, M. Hishida, K. Nagai, K. Teraoka, K. Kato, Suppressed proliferation of mouse osteoblast-like cells by a rough-surfaced substrate leads to low differentiation and mineralization, Mater. Sci. Eng. C. 30 (2010) 1–7. doi:10.1016/j.msec.2009.06.010.

[12] B.R. Coad, M. Jasieniak, S.S. Griesser, H.J. Griesser, Controlled covalent surface immobilisation of proteins and peptides using plasma methods, Surf. Coatings Technol. 233 (2013) 169–177. doi:10.1016/j.surfcoat.2013.05.019.

[13] J.H. Lee, H.W. Jung, I.-K. Kang, H.B. Lee, Cell behaviour on polymer surfaces with different functional groups, Biomaterials. 15 (1994) 705–711. doi:10.1016/0142-9612(94)90169-4.

[14] J.C. Ruiz, A. St-Georges-Robillard, C. Thérésy, S. Lerouge, M.R. Wertheimer, Fabrication and characterisation of amine-rich organic thin films: Focus on stability, Plasma Process. Polym. 7 (2010) 737–753. doi:10.1002/ppap.201000042.

[15] H. Kim, I.-S. Bae, S.-J. Cho, J.-H. Boo, B.-C. Lee, J. Heo, I. Chung, B. Hong, Synthesis and characteristics of NH2-functionalized polymer films to align and immobilize DNA molecules, Nanoscale Res. Lett. 7 (2012) 30. doi:10.1186/1556-276X-7-30.

[16] H. Iwase, H.-L. Chen, M.-C. Lin, C.-Y. Chen, C.-J. Su, S. Koizumi, T. Hashimoto, Nucleosome-like Structure from Dendrimer-Induced DNA compaction, Macromolecules. 45 (2012) 5208–5217. doi:10.1021/ma300308y.

[17] Y.-W. Yang, J.-Y. Wu, C.-T. Liu, G.-C. Liao, H.-Y. Huang, R.-Q. Hsu, M.-H. Chiang, J.-S. Wu, Fast incorporation of primary amine group into polylactide surface for improving C2 C12 cell proliferation using nitrogen-based atmospheric-pressure plasma jets., J. Biomed. Mater. Res. A. (2013) 160–169. doi:10.1002/jbm.a.34681.

[18] H.J. Griesser, R.C. Chatelier, T.R. Gengenbach, G. Johnson, J.G. Steele, Growth of human cells on plasma polymers: putative role of amine and amide groups., J. Biomater. Sci. Polym. Ed. 5 (1994) 531–554. doi:10.1163/156856294X00194.

[19] W. Hu, Q. Chen, H. Cai, Y. Zhang, The influences of processing parameters on structure of amine-containing film and its cell culture adsorption in pulsed DBD plasma, Thin Solid Films. 517 (2009) 4268–4271. doi:10.1016/j.tsf.2009.02.043.

[20] R.E. Ducker, M.T. Montague, G.J. Leggett, A comparative investigation of methods for protein immobilization on self-assembled monolayers using glutaraldehyde,

carbodiimide, and anhydride reagents., Biointerphases. 3 (2008) 59–65. doi:10.1116/1.2976451.

[21] M. Bashir, J.M. Rees, S. Bashir, W.B. Zimmerman, Microplasma copolymerization of amine and Si containing precursors, Thin Solid Films. 564 (2014) 186–194. doi:10.1016/j.tsf.2014.06.004.

[22] A. Harsch, J. Calderon, R.B. Timmons, G.W. Gross, Pulsed plasma deposition of allylamine on polysiloxane: A stable surface for neuronal cell adhesion, J. Neurosci. Methods. 98 (2000) 135–144. doi:10.1016/S0165-0270(00)00196-5.

[23] R.C. Ruaan, T.H. Wu, S.H. Chen, J.Y. Lai, Oxygen/nitrogen separation by polybutadiene/polycarbonate composite membranes modified by ethylenediamine plasma, J. Memb. Sci. 138 (1998) 213–220. doi:10.1016/S0376-7388(97)00237-8.

[24] A. Contreras-Garcia, M.R. Wertheimer, Low-pressure plasma polymerization of acetylene-ammonia mixtures for biomedical applications, Plasma Chem. Plasma Process. 33 (2013) 147–163. doi:10.1007/s11090-012-9409-5.

[25] F. Truica-Marasescu, P.-L. Girard-Lauriault, A. Lippitz, W.E.S. Unger, M.R. Wertheimer, Nitrogen-rich plasma polymers: Comparison of films deposited in atmospheric- and low-pressure plasmas, Thin Solid Films. 516 (2008) 7406–7417. doi:10.1016/j.tsf.2008.02.033.

[26] J. Kim, H. Park, D. Jung, S. Kim, Protein immobilization on plasma-polymerized ethylenediamine-coated glass slides, Anal. Biochem. 313 (2003) 41–45. doi:10.1016/S0003-2697(02)00563-8.

[27] C. Daunton, L.E. Smith, J.D. Whittle, R.D. Short, D.A. Steele, A. Michelmore, Plasma parameter aspects in the fabrication of stable amine functionalized plasma polymer films, Plasma Process. Polym. 12 (2015) 817–826. doi:10.1002/ppap.201400215.

[28] N. Inagaki, Plasma Surface Modification and Plasma Polymerization, 1st Editio, Taylor and Francis Group, 1996.

[29] K.V. Chan, I. Onyshchenko, A. Nikiforov, G. Aziz, R. Morent, N. De Geyter, Plasma polymerization of cyclopropylamine with a sub-atmospheric pressure DBD, Eur. Polym. J. 103 (2018) 1–10. doi:10.1016/J.EURPOLYMJ.2018.03.040.

[30] A. Manakhov, L. Zajíčková, M. Eliáš, J. Čechal, J. Polčák, J. Hnilica, Š. Bittnerová, D. Nečas, Optimization of cyclopropylamine plasma polymerization toward enhanced layer stability in contact with water, Plasma Process. Polym. 11 (2014) 532–544. doi:10.1002/ppap.201300177.

[31] S. Noel, B. Liberelle, L. Robitaille, G. De Crescenzo, Quantification of primary amine groups available for subsequent biofunctionalization of polymer surfaces, Bioconjug. Chem. 22 (2011) 1690–1699. doi:10.1021/bc200259c.

[32] L. Denis, P. Marsal, Y. Olivier, T. Godfroid, R. Lazzaroni, M. Hecq, J. Cornil, R. Snyders, Deposition of Functional Organic Thin Films by Pulsed Plasma Polymerization: A Joint Theoretical and Experimental Study, Plasma Process. Polym. 7 (2010) 172–181. doi:10.1002/ppap.200900131.

[33] A. Choukourov, H. Biederman, D. Slavinska, M. Trchova, A. Hollander, The influence of pulse parameters on film composition during pulsed plasma polymerization of

diaminocyclohexane, Surf. Coatings Technol. 174–175 (2003) 720–724. doi:10.1016/S0257-8972.

[34] N. De Geyter, R. Morent, C. Leys, Surface characterization of plasma-modified polyethylene by contact angle experiments and ATR-FTIR spectroscopy, Surf. Interface Anal. 40 (2008) 608–611. doi:10.1002/sia.2611.

[35] H.J.G. Thomas R. Gengenbach, Ronald C. Chatelier, Characterization of the Ageing of Plasma-deposited Polymer Films: Global Analysis of X-ray Photoelectron Spectroscopy Data, Surf. Interface Anal. 24 (1996) 271–281.

[36] A. Tarasova, P. Hamilton-Brown, T. Gengenbach, H.J. Griesser, L. Meagher, Colloid probe AFM and XPS study of time-dependent aging of amine plasma polymer coating in aqueous media, Plasma Process. Polym. 5 (2008) 175–185. doi:10.1002/ppap.200700054.

[37] G. Aziz, M. Thukkaram, N. De Geyter, R. Morent, Plasma parameters effects on the properties, aging and stability behaviors of allylamine plasma coated ultra-high molecular weight polyethylene (UHMWPE) films, Appl. Surf. Sci. 409 (2017) 381–395. doi:10.1016/j.apsusc.2017.03.027.

[38] K. Vasilev, L. Britcher, A. Casanal, H.J. Griesser, Solvent-induced porosity in ultrathin amine plasma polymer coatings, J. Phys. Chem. B. 112 (2008) 10915–10921. doi:10.1021/jp803678w.

[39] B. Finke, K. Schröder, A. Ohl, Structure retention and water stability of microwave plasma polymerized films from allylamine and acrylic acid, Plasma Process. Polym. 6 (2009) 70–74. doi:10.1002/ppap.200930305.

[40] G. Socrates, Infrared and Raman Characteristics Group Frequencies: Tables and Charts, Third, Wiley, 2004.

[41] M. Buddhadasa, C.R. Vandenabeele, R. Snyders, P.L. Girard-Lauriault, Single source precursor vs. precursor mixture for N-rich plasma polymer deposition: Plasma diagnostics and thin film analyses, Plasma Process. Polym. 14 (2017) 14–20. doi:10.1002/ppap.201700030.

[42] E.E. Johnston, B.D. Ratner, Surface characterization of plasma deposited organic thin films, J. Electron Spectros. Relat. Phenomena. 81 (1996) 303–317. doi:10.1016/0368-2048(95)02666-5.

[43] K.S. Siow, L. Britcher, S. Kumar, H.J. Griesser, Plasma methods for the generation of chemically reactive surfaces for biomolecule immobilization and cell colonization - A review, Plasma Process. Polym. 3 (2006) 392–418. doi:10.1002/ppap.200600021.

[44] H. Yasuda, T. Hirotsu, H.G. Olf, Polymerization of Organic Compounds Is an Electrodeless Glow Discharge - X. Internal Stress in Plasma Polymers., J. Appl. Polym. Sci. 21 (1977) 3179–3184. doi:10.1002/app.1977.070211128.

[45] C.-M. Chan, T.-M. Ko, H. Hiraoka, Polymer surface modification by plasmas and photons, Surf. Sci. Rep. 24 (1996) 1–54. doi:10.1016/0167-5729(96)80003-3.

[46] J.R. Jones, Observing cell response to biomaterials, Mater. Today. 9 (2006) 34–43. doi:10.1016/S1369-7021(06)71741-2.

[47] G. Ciapetti, E. Cenni, L. Pratelli, A. Pizzoferrato, In vitro evaluation of cell/biomaterial interaction by MTT assay, Biomaterials. 14 (1993) 359–364. doi:10.1016/0142-9612(93)90055-7.

[48] T. Mosmann, Rapid colorimetric assay for cellular growth and survival: Application to proliferation and cytotoxicity assays, J. Immunol. Methods. 65 (1983) 55–63. doi:10.1016/0022-1759(83)90303-4.

[49] D. Gerlier, N. Thomasset, Use of MTT colorimetric assay to measure cell activation, J. Immunol. Methods. 94 (1986) 57–63. doi:10.1016/0022-1759(86)90215-2.